NEURAL REGENERATION RESEARCH
www.nrronline.org

Research Article

Toxicities of amyloid-beta and tau protein are reciprocally enhanced in the *Drosophila* model

https://doi.org/10.4103/1673-5374.336872

Date of submission: August 3, 2021

Date of decision: October 10, 2021

Date of acceptance: December 15, 2021

Date of web publication: February 28, 2022

Zhen-Dong Sun[1, #], Jia-Xin Hu[1, #], Jia-Rui Wu[1, *], Bing Zhou[2, *], Yun-Peng Huang[1, *]

From the Contents

Graphical Abstract *In a Drosophila model of AD, amyloid β and tau protein reciprocally aggravate their toxicities to promote disease progression*

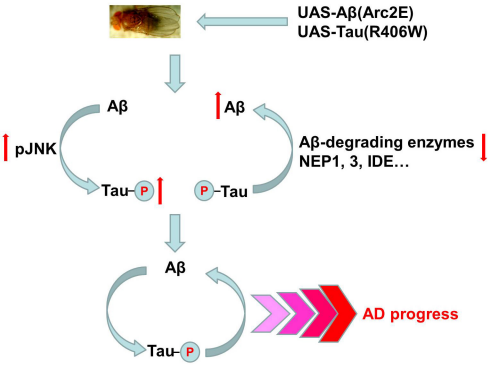

Abstract

Extracellular aggregation of amyloid-beta (Aβ) and intracellular tau tangles are two major pathogenic hallmarks and critical factors of Alzheimer's disease. A linear interaction between Aβ and tau protein has been characterized in several models. Aβ induces tau hyperphosphorylation through a complex mechanism; however, the master regulators involved in this linear process are still unclear. In our study with *Drosophila melanogaster*, we found that Aβ regulated tau hyperphosphorylation and toxicity by activating c-Jun N-terminal kinase. Importantly, Aβ toxicity was dependent on tau hyperphosphorylation, and flies with hypophosphorylated tau were insulated against Aβ-induced toxicity. Strikingly, tau accumulation reciprocally interfered with Aβ degradation and correlated with the reduction in mRNA expression of genes encoding Aβ-degrading enzymes, including *dNep1*, *dNep3*, *dMmp2*, *dNep4*, and *dIDE*. Our results indicate that Aβ and tau protein work synergistically to further accelerate Alzheimer's disease progression and may be considered as a combined target for future development of Alzheimer's disease therapeutics.

Key Words: Alzheimer's disease; amyloid-beta; amyloid-beta degradation; *Drosophila melanogaster*; c-Jun N-terminal kinase (JNK); neurodegeneration; tau; tau hyperphosphorylation

Introduction

Alzheimer's disease (AD) is the most common type of human dementia and causes memory loss, intellectual impairment, cognitive decline, language disability, and several other social disabilities. AD is predominantly categorized as sporadic AD, and only 5% of AD cases are caused by inherited mutations in proteins, such as amyloid beta precursor protein (APP), presenilin 1, and presenilin 2. Several risk factors have been suggested, including apolipoprotein E ε4 polymorphism, which is strongly correlated with AD pathology (Yamazaki et al., 2019), imbalance of the gut microbiota (Goyal et al., 2021), dyshomeostasis of trace metal elements (Lei et al., 2021), over-activation of microglia (Schwabe et al., 2020), and impaired exosomes (Zhang et al., 2021). Although some risk factors of sporadic AD have been characterized, the cause of sporadic AD remains unknown. Besides apolipoprotein E ε4, some genetic loci, such as phosphatidylinositol binding clathrin assembly protein and clusterin, are involved. Additionally, potential causes of AD include metabolic-related factors, such as hypercholesterolemia, type 2 diabetes, and hyperhomocysteinemia and inflammatory cues, such as neuro-inflammation and abnormal microglial activation (Ballatore et al., 2007; Chakrabarti et al., 2015). Characterization of core risk factors and axes for sporadic AD is paramount at present and will aid the further exploration of the mechanisms of sporadic AD.

Although the mechanism of AD is debated, AD can be pathologically characterized by the extracellular aggregation of amyloid beta (Aβ) plaques and intracellular tau tangles (Foidl et al., 2020; Mamun et al., 2020). Aβ is a short peptide composed of 39–42 amino acids that is generated and released from the amyloidogenic processing of APP by beta- and gamma-secretases (Chen et al., 2017). Aβ is the major component of senile plaques and is believed to be a cause of neuronal damage in the brains of AD patients (Chen et al., 2017; Zeng et al., 2021). Toxicity of Aβ has been investigated in multiple models (Chen et al., 2000; Newman et al., 2010; Prüßing et al., 2013). However, increasing evidence suggests that the microtubule-associated protein tau acts as the central player in AD pathology rather than Aβ (Bloom, 2014). Tau was initially characterized as a microtubule-associated protein that binds to and stabilizes microtubules. Under pathological conditions, such as AD and frontotemporal lobar degeneration, tau is hyperphosphorylated by several kinases, including microtubule affinity regulating kinase 2 (MARK2)\PAR-1, FYN, GSK3, and CDK5. Hyperphosphorylation of tau decreases microtubule binding affinity and axon localization, after which tau is released into the neuronal cell body and post-synaptic compartments. Subsequently, hyperphosphorylated tau forms oligomeric aggregates and tangles, which can further block the function of neurons and cause deleterious effects (Hoover et al., 2010; Srivastava et al., 2021).

According to the linear model of Aβ and tau interaction, Aβ disrupts neuronal function and induces tau dysregulation, and tau then acts as a downstream effector to execute Aβ toxicity; down-regulation of endogenous tau can effectively block Aβ toxicity (Bloom, 2014). Although some mediators, such as the FYN kinase and NMDA receptor, are suggested to be involved in the linear interaction process (Ittner et al., 2010; Bloom, 2014), the mechanism and the core mediators are still unclear.

[1]Key Laboratory of Systems Health Science of Zhejiang Province, Hangzhou Institute for Advanced Study, University of Chinese Academy of Sciences, Hangzhou, Zhejiang Province, China; [2]State Key Laboratory of Membrane Biology, School of Life Sciences, Tsinghua University, Beijing, China

*Correspondence to: Yun-Peng Huang, PhD, huangyp@ucas.ac.cn; Bing Zhou, PhD, zhoubing@mail.tsinghua.edu.cn; Jia-Rui Wu, PhD, wujr@sibs.ac.cn.
https://orcid.org/0000-0003-4116-7934 (Yun-Peng Huang); https://orcid.org/0000-0002-6585-9284 (Bing Zhou); https://orcid.org/0000-0002-3065-5599 (Jia-Rui Wu)
#These two authors contributed equally to this paper.

Funding: *This study was supported by the National Basic Research Program of China, Nos. 31700883 (to YPH) and 91649118 (to BZ), China Postdoctoral Science Foundation, No. 2015M581072 (to YPH), and the Strategic Priority Research Program of the Chinese Academy of Sciences, No. XDB38000000 (to JRW).*

How to cite this article: *Sun ZD, Hu JX, Wu JR, Zhou B, Huang YP (2022) Toxicities of amyloid-beta and tau protein are reciprocally enhanced in the Drosophila model. Neural Regen Res 17(10):2286-2292.*

Drosophila melanogaster (*D. melanogaster*) is widely used in studies of human neurodegenerative diseases (Bilen and Bonini, 2005). The majority of fundamental biological pathways are conserved between the fly and human genomes according to comparative genomics studies, and nearly 70% of human disease-related genes have orthologs in the fly genome (Fortini et al., 2000). Compared with other model organisms, *D. melanogaster* offers many advantages, such as a short lifespan, an abundance of genetic tools, and easy access for phenotypic characterization. These advantages can benefit the analyses of fundamental molecular and pathological mechanisms in complex human diseases, including human neurodegenerative diseases (Bilen and Bonini, 2005).

At present, various human neurodegenerative diseases can be modeled in *D. melanogaster*, including AD, Parkinson's disease, Huntington's disease, and amyotrophic lateral sclerosis. Expression of human $A\beta_{42}$ or tau in the fly central nervous system (CNS) can be used to investigate some of the pathological features of human AD, such as cognitive decline, behavioral dysfunction, pathological aggregate formation, reduction of synaptic transmission and neuronal mitochondrial homeostasis, and shortened lifespan (Link, 2005; Prüßing et al., 2013). Indeed, the *D. melanogaster* AD model has been widely used to dissect the fundamental mechanisms of AD (Wittmann et al., 2001; Shulman and Feany, 2003; Folwell et al., 2010; Sowade and Jahn, 2017; Jeon et al., 2020). In this study, we used the *Drosophila* model to further investigate the relationship between Aβ and tau. Our results suggest that Aβ and tau can reciprocally aggravate their toxicities to promote AD progression.

Materials and Methods

Fly stocks and crosses

The Aβ fly line used in this study was UAS-Aβ(Arc2E) (designated as Aβ*) and was obtained from Tsinghua University (Beijing, China). The tau fly line was UAS-Tau(R406W) (designated as Tau*). The tau mutant line Tau(S2A) was UAS-Tau(R406W, S262A, S356A) (designated as Tau*S2A). The UAS-Tau(R406W) and UAS-Tau(R406W, S2A) flies were obtained from Stanford University (Palo Alto, CA, USA). The wild-type control, GMR-Gal4, and ELAV-Gal4 flies were previously purchased from the Bloomington *Drosophila* Stock Center (Indiana University; Bloomington, IL, USA). The GMR-Gal4\Sm6a; UAS-Tau(R406W)\Tm6B flies and GMR-Gal4; UAS-Tau(R406W, S2A)\Sm6a fly crosses were generated as previously described (Huang et al., 2015). Similarly, ELAV-Gal4 flies were crossed with UAS-Tau(R406W) and UAS-Tau(R406W, S2A) flies to obtain ELAV-Gal4\Y; UAS-Tau(R406W)\Tm6B and ELAV-Gal4\Y; UAS-Tau(R406W, S2A)\Sm6a flies. These flies were then crossed with UAS-Aβ(Arc2E) flies to obtain GMR-Gal4\UAS-Aβ(Arc2E); UAS-Tau(R406W)\+, GMR-Gal4, UAS-Tau(R406W, S2A)\UAS-Aβ(Arc2E), ELAV-Gal4\+; UAS-Aβ(Arc2E)\+; UAS-Tau(R406W)\+, and ELAV-Gal4\+; UAS-Aβ(Arc2E)\UAS-Tau(R406W, S2A) flies. The GMR-Gal4\UAS-GFP and ELAV-Gal4\+; UAS-GFP\+ flies were used as controls (**Table 1**). Flies were maintained on a standard corn-based medium at 25°C. The c-Jun kinase (JNK) inhibitor SP600125 (Cat# S5567, MilliporeSigma, Burlington, MA, USA) was added to the medium at a final concentration of 10 μM. Vitamin C (Cat# 50-81-7, Sinopharm, Shanghai, China) was added to the medium at a final concentration of 5 mM to reduce the level of reactive oxygen species (ROS).

Table 1 | **Fly information**

Flies #	Genotypes	Inserted chromosomes
Fly stock with tau(R406W) expression in fly compound eyes	GMR-Gal4\Sm6a; UAS-Tau(R406W)\Tm6B	2; 3
Fly stock with tau(R406W, S2A) expression in fly compound eyes	GMR-Gal4, UAS-Tau(R406W, S2A)\Sm6a	2
Fly stock with tau(R406W) expression in fly CNS	ELAV-Gal4\Y; UAS-Tau(R406W)\Tm6B	X; 3
Fly stock with tau(R406W, S2A) expression in fly CNS	ELAV-Gal4\Y; UAS-Tau(R406W, S2A)\Sm6a	X; 2
Aβ(Arc2E) and tau(R406W) co-expressed in fly compound eyes	GMR-Gal4\UAS-Aβ(Arc2E); UAS-Tau(R406W)\+	2; 3
Aβ(Arc2E) and tau(R406W, S2A) co-expressed in fly compound eyes	GMR-Gal4, UAS-Tau(R406W, S2A)\UAS-Aβ(Arc2E)	2
Aβ(Arc2E) and tau(R406W) co-expressed in fly CNS	ELAV-Gal4\+; UAS-Aβ(Arc2E)\+; UAS-Tau(R406W)\+	X; 2; 3
Aβ(Arc2E) and tau(R406W, S2A) co-expressed in fly CNS	ELAV-Gal4\+; UAS-Aβ(Arc2E)\UAS-Tau(R406W, S2A)	X; 2
Control fly for GMR-Gal4 driven phenotypes	GMR-Gal4\UAS-GFP	2
Control fly for ELAV-Gal4 driven phenotypes	ELAV-Gal4\+; UAS-GFP\+	X; 2

CNS: Central nervous system.

Observations of *Drosophila* eye phenotypes and scanning electron microscopy (scanning-EM)

The rough eye phenotype was observed and quantified according to severity (Crowther et al., 2005; Oh et al., 2015). Representative photographs were captured using an XTL-165-MT microscope (Phenix; Jiangxi, China). The rough eye phenotype was divided into four groups for quantification as follows: severe: +++, medium: ++, slight: +, and normal: –. The numbers of corresponding rough eye phenotypes were counted and analyzed. For the scanning-EM observations, adult flies were quickly frozen in liquid nitrogen and adhered to the scanning-EM objective table. Images of fly eyes were observed using the FEI Quanta 2000 Scanning Electron Microscope (FEI Company, Hillsboro, OR, USA) as described previously (Huang et al., 2014) under the following conditions: voltage, 15 kV; pressure, 300 Pa; and 4°C with 36.9% humidity.

Climbing ability assay and lifespan analyses

To determine climbing ability (Madabattula et al., 2015), newly eclosed female flies were collected and divided into three to six individual groups, and each group included 20 adult flies. Flies were aged at 25°C for 3–4 weeks, and the numbers of flies that climbed 3 cm in 8 seconds were manually counted and divided by the total number of flies, which was then used as the climbing index (%). To record fly lifespans, newly eclosed flies were collected and maintained at 25°C, fly food was exchanged every 2 days, and the numbers of dead flies were counted. For each genotype, at least 80–100 newly eclosed flies were used to record lifespans.

Separation of soluble and insoluble protein fractions and western blots

To separate the soluble and insoluble tau fractions, 50 adult fly heads were collected, homogenized in NP40 protein extraction buffer (Beyotime; Cat# P0013; Shanghai, China), and centrifuged at 12,000 × *g* for 10 minutes. The supernatant was centrifuged again at 100,000 × *g* for 30 minutes and then collected as the soluble fraction. The pellet was resuspended in NP40 protein extraction buffer containing 1% SDS (Cat# A100227, Sangon Biotech, Shanghai, China) and collected as the insoluble fraction. Protein samples were mixed with 5× SDS-loading buffer, denatured at 37°C for 30 minutes, and loaded on 12% SDS-polyacrylamide gel electrophoresis (SDS-PAGE) gels (Cat# B546013, Sangon Biotech) to separate proteins. The separated proteins were transferred on to a 0.22 μm polyvinylidene fluoride membrane (Cat# ISEQ00010, Millipore, Shanghai, China). The membrane was hybridized for 12 hours with mouse anti-tau antibody (clone Tau-5; 1:1500 dilution; Innovative Research Cat# AHB0042, RRID: AB_1502093, Thermo Fisher Scientific; Waltham, MA, USA) and rabbit anti-tubulin antibody (1:2000 dilution; Cat# ab6046, RRID: AB_2210370, Abcam, Cambridge, MA, USA) and rinsed three times with 1× phosphate-buffered saline containing 0.1% Tween 20. The blot was then hybridized with the corresponding secondary antibodies for 2 hours (horseradish peroxidase [HRP]-conjugated rabbit anti-mouse IgG, 1:2000, Cat# 7076S, RRID: AB_330924 and HRP-conjugated goat anti-rabbit IgG, 1:2000, Cat# 7074S, RRID: AB_2099233; both from Cell Signaling Technology; Shanghai, China). The immunoblot signals were observed using enhanced chemiluminescence (Cat# 34075, Thermo Fisher Scientific). Western blot results were analyzed and quantified using ImageJ software (v1.8.0, National Institutes of Health, Bethesda, MD, USA; Schneider et al., 2012), and the levels of soluble and insoluble tau were normalized to β-tubulin levels.

To separate soluble and insoluble Aβ fractions, 50 adult fly heads were collected. The soluble fraction was collected using the NP40 protein extraction buffer after centrifugation at 100,000 × *g* for 30 minutes as described above. To dissolve the Aβ aggregates and collect the insoluble fraction, NP40 extraction buffer was mixed with formic acid to obtain a 70% formic acid extraction buffer, which was used to dissolve the pellets. The samples were sonicated for 2 minutes to break up Aβ aggregates using a JY92-IIDN sonicator (HUXI Company, Shanghai, China). Soluble and insoluble Aβ fractions were mixed with 5× SDS-loading buffer and loaded onto 15% SDS-PAGE gels. Western blotting was performed as described above using rabbit anti-Aβ antibody (1:1000, Cat# 14974P, RRID: AB_2798671, Cell Signaling Technology), mouse anti-β-actin (1:2000, Cat# TA-09, RRID: AB_2636897, ZSGB-Bio, Beijing, China), and the corresponding secondary antibodies (HRP-conjugated rabbit anti-mouse IgG and goat anti-rabbit IgG as described above). Western blots were analyzed and quantified as described above, and the levels of soluble and insoluble Aβ were normalized to β-actin levels.

To detect tau phosphorylation and JNK activation, at least 25 adult fly heads were collected and homogenized in NP40 protein extraction buffer containing proteinase and phosphatase inhibitors. After centrifuging for ten minutes at 12,000 × *g*, the supernatant was mixed with 5× SDS-loading buffer and denatured. The proteins were separated and blotted as described above. The signal for phosphorylated (p)-JNK was normalized to total JNK. The phosphorylated tau signals (pS262, PHF-1, and AT8) were normalized to total tau signals using ImageJ software. The following antibodies were used: mouse anti-AT8 antibody (1:1500 dilution; a gift from Stanford University, Palo Alto, CA, USA); mouse anti-PHF-1 antibody (1:2000 dilution; Developmental Studies Hybridoma Bank; University of Iowa; Iowa City, IA, USA); rabbit anti-pS262 (1:1000; Cat# 44-750G, RRID: AB_2533743, Thermo Fisher Scientific), rabbit anti-JNK (1:1500 dilution, Cat# sc-571, RRID: AB_632385, Santa Cruz Biotechnology, Santa Cruz, CA, USA), anti-p-JNK (rabbit, 1:2000, Cat# 4668P, RRID: AB_823588; Cell Signaling Technology). For these western blot experiments, the primary antibodies were incubated for 12 hours at 4°C; the secondary antibodies were incubated for 2 hours at room temperature.

To analyze tau phosphorylation in mammalian cells, a pcDNA3.1 plasmid construct with Tau(R406W)-RFP sequences (designated as Tau*-RFP) was transfected into HEK293 cells (obtained from the National Collection of Authenticated Cell Culture; Shanghai, China) to generate cell lines with Tau*-RFP expression. The pcDNA3.1 vector alone was transfected to generate a control cell line. Cells were treated with 10 μM $A\beta_{40}$ peptide for 24 hours and

harvested for western blot analysis. The levels of tau phosphorylation and p-JNK were analyzed by western blot as described above, and the signals were normalized to Tau5 or JNK respectively, using ImageJ software.

RNA extraction and gel-based reverse transcription PCR analysis

Gel-based reverse transcription PCR (RT-PCR) (Mitchell and Iadarola, 2010) was used to analyze the mRNA expression level of Aβ-degrading enzymes (**Additional Table 1**). For fly RNA extraction, 30 adult fly heads were collected and homogenized in Trizol buffer (Thermo Fisher Scientific). The cDNA was synthesized using a reverse transcription kit (Cat# AE311; TransGen Biotech; Beijing, China). For the calculation and quantification of RT-PCR results, RT-PCR samples were separated on 1.5% agarose gels (Cat# A620014, Sangon Biotech), and the intensity of the DNA bands was evaluated using ImageJ software and normalized to the intensity of the band for ribosomal protein 49 (rp49), which was used as the loading control (Cerro-Herreros et al., 2017). Primer sequences used for RT-PCR analysis of *dNep1*, *dNep2*, *dNep3*, *dIDE*, and *rp49* were previously described (Lang et al., 2013), and the primer sequences for *dBace*, *dMmp1*, *dMmp2*, *dNep4*, *dNepl21*, *dNepl7*, and *dAnce* were obtained from the *Drosophila* primer Bank (Hu et al., 2013) (DRSC Fly Primer Bank: https://www.flyrnai.org/flyprimerbank). The primer sequences are listed in **Table 2**.

Table 2 | **Primer sequences used for reverse transcription PCR**

Gene	Primer sequence (5'–3')	Product size (bp)
dNep1	F: GAT GAC GCA GGG CGA GAA	146
	R: TGG GCG TAG TTG AGA AAG AAC A	
dNep2	F: CCG CAG ATG GGC TGA GAA	148
	R: TGC ACG CCG GTA GTA ATA CG	
dNep3	F: GTC CAG CCG CAC CAA AAA	146
	R: CCA TTG ATT GCA GGA ATA TCC A	
dIDE	F: AAA GAG GGA CCC AAG AAG TG	122
	R: ATA TTT GCA TGG ACG AGA CG	
dBace	F: AGG AGC AGA ACT TTG TGA AGA C	129
	R: AAG CCA TAT TCA TCG AGT TGG AC	
dPsn	F: ATG CGT GAA CCT TGT GGC T	142
	R: AGA CGG GGA CGA ATA ACT TGA	
dAnce	F: CGC GAG TTC TAC GAC AAG GC	271
	R: GTG CAT GGG AAT GGG TCC TG	
dMmp2	F: ACT TTG ACG GCG AAT CCG AT	554
	R: GGA TTC CTC TCC CAC TGG CT	
dNepl7	F: CTG GCC AGT GCT CAA TCA AT	351
	R: ATG CCA GTT TGG TCT TAG CC	
dMmp1	F: CTT CGC GGG ACT GAA CAT CA	159
	R: TAG GTG AGG TTC TTC ACA CGC	
dNepl21	F: CCC ACG ATT CCC ACG ACA C	209
	R: GTA TCG GTA GGC CAT GCG A	
dNep4	F: TGG TAA TGC TGC CAC TGA CCC	486
	R: CGC GGC GCT CCC GTA TTC TGA	
rp49	F: GCA CCA AGC ACT TCA TCC	252
	R: CGA TCT CGC CGC AGT AAA	

F: Forward; R: reverse.

Statistical analysis

Biochemical analyses were blinded to fly genotypes and treatments, whereas the fly phenotyping was not blinded to the experimental conditions. The data are presented as the mean ± SEM. Differences among groups were analyzed by GraphPad Prism, version 8.0.1 for Windows (GraphPad Software, Inc., San Diego, CA, USA). Unpaired *t*-tests were used for comparisons of two groups, and one-way ANOVA was used for comparison of multiple groups and to compare the means of pre-selected pairs of columns. $P < 0.05$ was considered statistically significant.

Results

Aβ expression aggravates tau protein toxicity in the *Drosophila* model

To investigate the influence of Aβ on tau protein toxicity in the fly model, we co-expressed UAS-Aβ(Arc2E), a more toxic mutant of Aβ, and UAS-Tau(R406W) (designated as Aβ* and Tau*, respectively) in *Drosophila* compound eyes by using the GMR-Gal4 driver (**Additional Figure 1A**, model preparation). Tau* expression caused the rough eye phenotype because of its toxic effect on photoreceptor neurons, and Aβ* co-expression further aggravated this phenotype. We classified the rough eye phenotypes into four groups according to severity. Tau* expression alone caused medium rough eyes, whereas Aβ* expression alone did not result in a rough eye phenotype at 25°C. The co-expression of Aβ* and Tau* increased the ratio of severe rough eyes from approximately 30% to 80% (**Figure 1A** and **B**). These results suggested that Aβ aggravated tau protein toxicity. To confirm this result, we investigated the fly eye phenotype using the scanning-EM microscope and found that the rough eye phenotype caused by Tau* expression was exacerbated by co-expression of Aβ* (**Figure 1C**). The severity of the fusion of ommatidia, dents in the retina, and reduced eye size of Tau* flies was exacerbated by Aβ* expression (Prüßing et al., 2013).

Tau expression not only causes rough eyes in *D. melanogaster*, it also shortens the lifespan and reduces climbing ability (Gistelinck et al., 2012). Therefore, we evaluated the lifespan and climbing ability of Tau* and Aβ*\Tau* flies by using the ELAV-Gal4 driver (**Additional Figure 1B**, model preparation). Aβ* expression further reduced the medium lifespan of Tau* flies (**Figure 1D**); the medium lifespan (50% survival) for Tau* flies was reduced from approximately 37 to 25 days after co-expression of Aβ* (**Figure 1D**). As a control, the medium lifespan for Aβ* flies was approximately 33 days (**Figure 1D**). The climbing ability assay also showed similar trends. Aβ* co-expression significantly reduced the climbing ability of Tau* flies; the climbing index was reduced from 60% for Tau* flies compared with 8% for Aβ*\Tau* flies (**Figure 1E**). As a control, the climbing index for Aβ*-expressing flies was 40%. The above results suggested that tau protein toxicity was significantly aggravated by Aβ.

Aβ aggravates tau protein hyperphosphorylation and accumulation

Because hyperphosphorylation is the major driving force for tau polymerization and toxicity, we analyzed tau phosphorylation using phosphorylation-specific antibodies, especially to detect the AD pathology-related phosphorylated epitopes, such as Ser396\Ser404 (PHF-1 epitope), Ser202\Thr205 (AT8 epitope), and Ser262. Typically, Ser262 is one of the regulatory phosphorylation sites of tau protein, which mediates subsequent tau hyperphosphorylation on PHF-1(Ser396, Ser404) and Ser202 (Rissman et al., 2004; Nishimura et al., 2004).

Our western blot results demonstrated that Aβ* expression significantly increased the level of tau hyperphosphorylation in Tau* flies; phosphorylation levels on Ser262, PHF-1, and AT8 epitopes all increased when Aβ* was co-expressed with Tau* (**Figure 2A** and **B**). Ser262 and PHF-1 signals were also significantly increased in Tau*-RFP cells treated with $Aβ_{40}$ peptide (**Figure 2C** and **D**), indicating Aβ can significantly increase tau hyperphosphorylation. We determined the total levels of tau protein in Aβ*\Tau* flies through the separation and analysis of the soluble and insoluble tau fractions. Aβ* co-expression significantly increased the level of soluble and insoluble tau protein (**Figure 2E** and **F**), indicating that Aβ can exacerbate tau accumulation and hyperphosphorylation as well as toxicity.

Tau hyperphosphorylation mediates the toxicity of Aβ

To further confirm the effect of Aβ on tau hyperphosphorylation, we used Tau*S2A flies that expressed a hypophosphorylated tau mutant. Tau*S2A flies carry alanine substitutions on both Ser262 and Ser356 tau, which are the regulatory sites for tau phosphorylation. These mutations can dramatically reduce the subsequent phosphorylation of several other pathologically-related phosphorylation sites, including PHF-1 (Nishimura et al., 2004).

Using UAS-Tau*S2A and UAS-Aβ* flies, we further analyzed the influence of Aβ on the toxicity of TauS2A. Strikingly, Aβ* co-expression did not worsen the phenotype of Tau*S2A flies. The rough eye phenotype of Tau*S2A flies was not affected when Aβ* was co-expressed. As a comparison, the rough eye phenotype of Tau* flies was more severe (**Figure 3A** and **B**). Moreover, when the fly climbing ability was analyzed, the climbing abilities of Aβ*\Tau*S2A and Aβ* flies were similar (**Figure 3C**), suggesting that Aβ was unable to worsen the toxicity of TauS2A. Results from fly longevity assays also supported this conclusion. The lifespan of Aβ* flies was similar to that of Tau*S2A and Aβ*\Tau*S2A flies (**Figure 3D**). The above results indicated that the hypophosphorylated tau mutant was unaffected by Aβ. TauS2A could not execute the toxicity of Aβ, which suggests hyperphosphorylated tau is a critical mediator of Aβ toxicity.

The influence of Aβ on tau toxicity is partly dependent on JNK

Although several kinases and phosphatases control tau phosphorylation, the kinase that mediates the linear interaction between Aβ and tau is still unclear. JNK is one of the kinases activated by Aβ and contributes to tau Ser262 and PHF-1 phosphorylation (Yao et al., 2005; Tatebayashi et al., 2006; Dias-Santagata et al., 2007; Ploia et al., 2011). Therefore, we suspected that JNK may mediate the effects of Aβ on tau protein. This indeed appeared to be the case. First, western blots demonstrated that Aβ* co-expression activated JNK in Tau* flies (**Figure 4A** and **B**). $Aβ_{40}$ peptide treatment also activated JNK in Tau*-RFP cells (**Additional Figure 2A** and **B**). Second, when SP600125 was used to inhibit JNK activity, we found that JNK inhibition significantly alleviated the severe rough eye phenotype of Aβ*\Tau* flies (**Figure 4C** and **D**). Similar treatment blocked JNK activation in Aβ* flies (**Figure 4E** and **F**) and Aβ-induced tau hyperphosphorylation (**Figure 4G** and **H**), indicating that the inhibition of JNK blocked Aβ-induced tau toxicity. Our results suggest that JNK is one of the kinases that mediates the linear interaction between Aβ and tau.

Tau increases Aβ accumulation in the fly model

To further investigate the interaction between Aβ and tau toxicity, we tested the levels of soluble and insoluble Aβ in Aβ*\Tau* flies. Surprisingly, compared with levels in Aβ* flies, levels of soluble and insoluble Aβ were elevated in Aβ*\Tau* flies (**Figure 5A** and **B**), indicating that tau aggravated Aβ accumulation. We further tested whether Aβ degradation was interrupted. The proteases neprilysin 1–3 (NEP1, 2, 3), endothelin-converting enzyme 1\2 (ECE1\2), angiotensin-converting enzyme (ACE), matrix metalloproteinases (Mmps), and insulin-degrading enzyme (IDE) have been reported to be involved in the Aβ degradation process (Qiu et al., 1998; Carson and Turner,

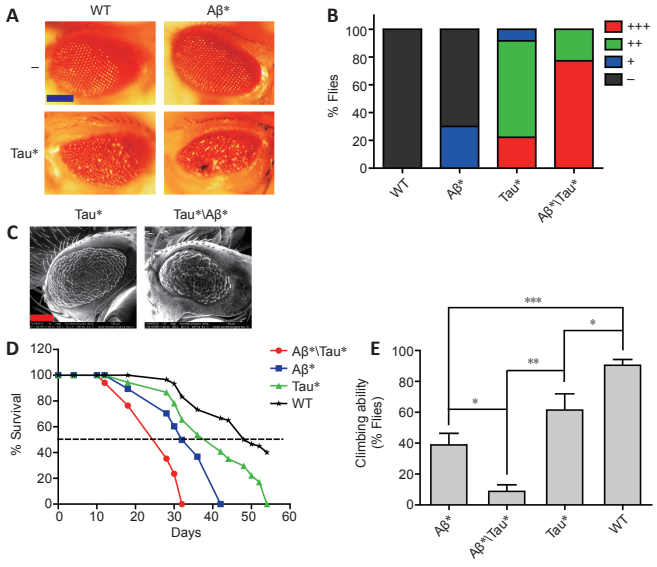

Figure 1 | **Amyloid-beta (Aβ) expression enhances tau protein toxicity in the *Drosophila* model.**
(A) Images of the compound eyes from Tau* flies [GMR-Gal4>UAS-Tau(R406W)]. GMR-Gal4 was used to drive Tau* and Aβ* expression in the eyes. Scale bar: 100 μm. (B) Quantitation of rough eye phenotypes in panel A. +++: severe rough eye; ++: medium rough eye; +: mild rough eye; –: normal eye. The number of flies used for eye phenotype calculations was as follows: wild-type (WT) flies, 50; Aβ(Arc2E) flies (Aβ*), 38; Tau(R406W) flies (Tau*), 36; Aβ(Arc2E) and Tau(R406W) co-expression (Aβ*\Tau*), 44 flies. (C) Scanning electron microscopy (EM) images of the compound eyes from Tau* and Aβ*\Tau* flies. Scale bar: 100 μm. For each genotype, four adult flies were randomly chosen and quickly frozen in liquid N_2. Scanning-EM images were collected under the following conditions: voltage, 15 kV; pressure, 300 Pa; 4°C with 36.9% humidity. For Figure 1C, scanning-EM images of the rough eye phenotype are shown. The rough eye phenotype was observed and evaluated according to the fusion of ommatidia, dents in the retina, and reduced eye size. (D) The lifespans for Tau* flies and Aβ*\Tau* flies. ELAV-Gal4 was used to drive Tau* and Aβ* expression in the fly central nervous system (CNS). The number of flies used for lifespan analyses: Aβ*\Tau* flies, 102; Aβ* flies, 114; Tau* flies, 108; WT flies, 116. (E) Climbing ability of different lines of flies. ELAV-Gal4 was used to drive Tau* and Aβ* expression in the CNS. Data are presented as the mean ± SEM. $*P < 0.05$, $**P < 0.01$, $***P < 0.001$ (unpaired *t*-test).

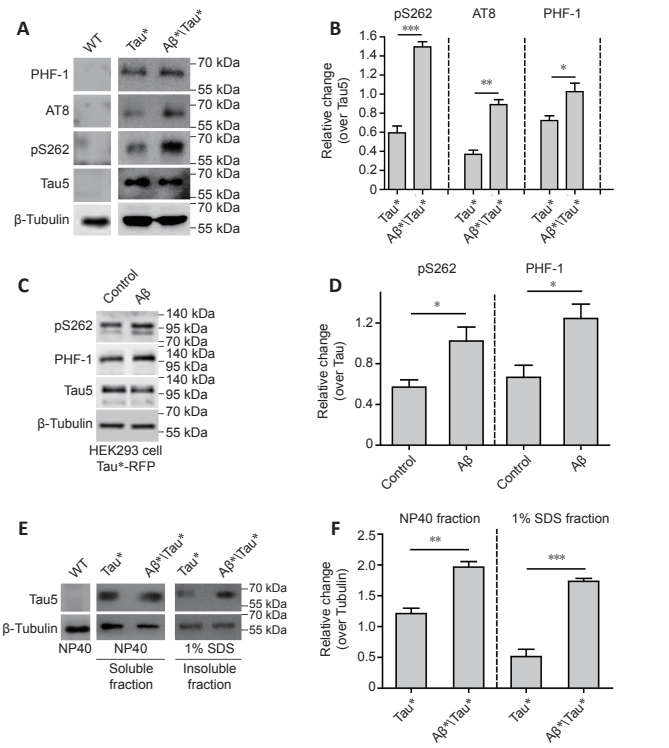

Figure 2 | **Amyloid-beta (Aβ) aggravates tau protein hyperphosphorylation and accumulation.**
(A) Western blot analysis of tau phosphorylation using phosphorylation site-specific antibodies. Protein extracts were prepared from 25 adult fly heads. ELAV-Gal4 was used to drive Tau* and Aβ* expression in the fly central nervous system (CNS). Tubulin was used as a loading control. (B) The quantitative results for panel A. The pS262, PHF-1, and AT8 levels were normalized to the Tau-5 antibody signal. (C) Western blot analysis of tau hyperphosphorylation in HEK293 cells with Tau*-RFP expression. Tau*-RFP cells were treated with 10 μM $Aβ_{40}$ peptide for 24 hours. Tubulin was used as the loading control. (D) The quantitative results for panel C. Western blot results were calculated using ImageJ software. Levels of pS262 and PHF-1 were normalized to tau5. (E) Western blot analysis of the levels of soluble and insoluble tau protein. Tubulin was used as the loading control. Protein extracts were prepared from 50 adult fly heads. ELAV-Gal4 was used to drive Tau* and Aβ* expression in the fly CNS. (F) The quantitative results for panel E. The tau protein level was normalized to tubulin. Data are presented as the mean ± SEM. $*P < 0.05$, $**P < 0.01$, $***P < 0.001$ (unpaired *t*-test). All western blot analyses were performed three times, and representative blots are shown.

2002; Miners et al., 2008). Therefore, we evaluated the mRNA expression levels of Aβ-degrading enzymes in the flies (**Additional Table 1**). The RT-PCR results showed that the expression levels of *Drosophila Nep1*, *Nep3*, *Mmp2*, *Nepl7*, and *IDE* were reduced in Aβ*\Tau* flies (**Figure 5C** and **D**), while the levels of *Nep2*, *Mmp1*, *Nepl21*, and *Ance* were unchanged (**Figure 5C** and **D**). These results indicated that tau intensified Aβ accumulation, which correlated with the inhibition of the expression of Aβ-degrading enzymes.

Our results indicated that the toxicity of Aβ and tau was reciprocally aggravated. The toxicity of Aβ was dependent on tau hyperphosphorylation. Aβ expression resulted in the hyperphosphorylation and accumulation of tau via JNK activation. Tau also blocked the mRNA expression of Aβ-degrading enzymes, such as *dNep1*, *dNep3*, *dMmp2*, *dNep4*, and *dIDE*, which subsequently exacerbated Aβ accumulation and toxicity (**Figure 5E**). This interaction loop will further deteriorate AD pathology.

Discussion

At the early stage of AD, Aβ is considered to be an initiating element (Bloom, 2014), which triggers the dysfunction of synapses. Subsequently, normal tau proteins are converted into hyperphosphorylated and pathological forms, leading to changes in tau localization, distribution, and aggregation (Zempel et al., 2010). In this cascade, tau proteins act as the downstream effectors of Aβ toxicity. Increasing evidence indicates that the toxicity of Aβ is largely dependent on tau (Bloom, 2014). Tau pathology correlates well with the neurodegenerative process and cognitive decline in AD, and, typically, tau deficiency can substantially eliminate Aβ toxicity in animal models (Ittner et al., 2010; Ossenkoppele et al., 2016). Our study further suggests that Aβ toxicity is dependent on tau hyperphosphorylation. Therefore, AD may be considered as a form of Aβ-facilitated tauopathy: Aβ triggers tau dysregulation and toxicity (van der Kant et al., 2020).

To understand the Aβ-tau cascade, it is critical to characterize the mediators. Our results indicated that the Aβ-mediated increase in tau toxicity was partly dependent on JNK. This phenomenon was also found in other models (Wei et al., 2002; Yao et al., 2005; Ma et al., 2009). Importantly, JNK can phosphorylate tau protein on the phospho-epitopes related to AD pathology, including Ser262, Ser396, and Ser404 (Goedert et al., 1997; Yoshida et al., 2004; Cao et al., 2013; Tyagi et al., 2013). JNK is correlated with AD pathology; it is redistributed and activated in AD and is associated with neuronal neurofibrillary tangles (Hensley et al., 1999; Zhu et al., 2001;

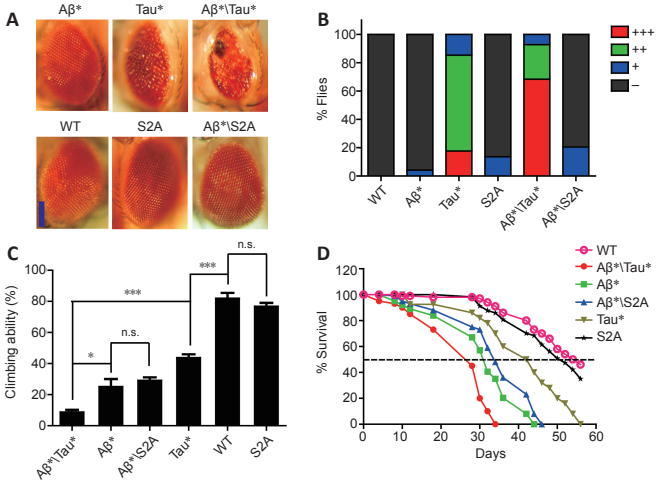

Figure 3 | **Hypophosphorylated mutant tau protein is resistant to amyloid-beta (Aβ).**
(A) Images of fly compound eyes. GMR-Gal4 was used to drive Tau(R406W) (designated as Tau*), Tau*(S2A), and Aβ(Arc2E) (designated as Aβ*) expression in fly eyes. Scale bar: 100 μm. (B) The quantitative results for rough eye phenotypes presented in panel A. +++: Severe rough; ++: medium rough; +: mild rough; –: normal. The number of flies used for eye phenotype calculations: wild-type (WT) flies, 50; Aβ* flies, 48; Tau* flies, 34; Tau*(S2A) flies, 44; Aβ*\Tau* flies, 41; Aβ*\Tau*(S2A) flies, 44. (C) Climbing ability of Tau*(S2A) and Tau* flies. ELAV-Gal4 was used to drive Tau*(S2A), Tau*, and Aβ* expression in the fly central nervous system (CNS). Data are presented as the mean ± SEM. $*P < 0.05$, $**P < 0.01$, $***P < 0.001$ (unpaired *t*-test). (D) Lifespans of Tau* and Tau*(S2A) flies. ELAV-Gal4 was used to drive Tau*, Tau*(S2A), and Aβ* expression in the fly CNS.

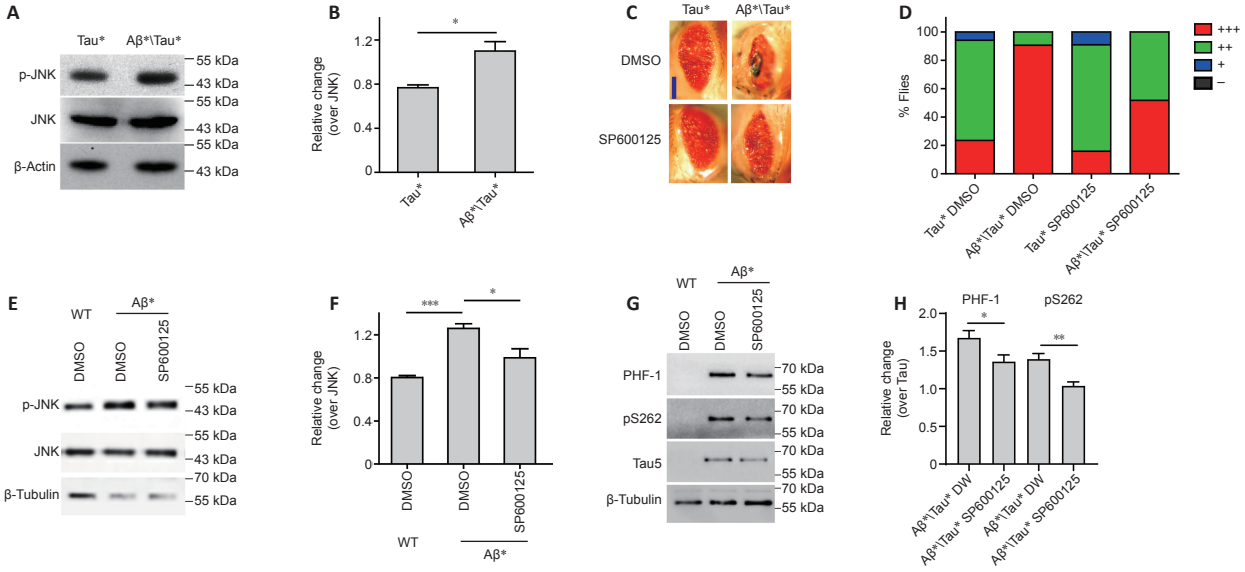

Figure 4 | **Amyloid-beta (Aβ) aggravates tau protein toxicity via JNK activation.**
(A) Representative western blot (WB) showing the level of phosphorylated (p) c-Jun N-terminal kinase (JNK). Protein extracts were prepared from 25 adult fly heads; ELAV-Gal4 was used to drive Tau(R406W) (designated as Tau*) and Aβ(Arc2E) (designated as Aβ*) expression in the fly central nervous system (CNS). Actin was used as the loading control. (B) The quantitative results for panel A; p-JNK level was normalized to JNK. (C) Images of fly compound eyes. GMR-Gal4 was used to drive Tau* and Aβ* expression in fly eyes; 10 μM SP600125 was used to inhibit JNK activity. Scale bar: 100 μm. (D) The quantitative results for panel C. +++: severe rough eye; ++: medium rough eye; +: mild rough eye; –: normal eye. The number of flies used for eye phenotype calculations: DMSO-treated Tau* flies, 34; SP60015-treated Tau* flies, 32; DMSO-treated Aβ*\Tau* flies, 44; SP600125-treated Aβ*\Tau* flies, 29. (E) Representative WB analysis of the level of p-JNK in SP600125-treated Aβ* flies. Protein extracts were prepared from 25 adult fly heads. ELAV-Gal4 was used to drive Aβ* expression in the fly CNS. Tubulin was used as the loading control. (F) The quantitative results for panel E; the p-JNK level was normalized to JNK. (G) Representative WB analysis of tau hyperphosphorylation in SP600125-treated flies. Protein extracts were prepared from 25 adult fly heads. ELAV-Gal4 was used to drive Tau* and Aβ* expression in the fly CNS. Tubulin was used as the loading control. (H) The quantitative results for panel G; pS262 and PHF-1 signals were normalized to the Tau-5 antibody signal. All WBs were repeated three times. Data are presented as the mean ± SEM. $*P < 0.05$, $**P < 0.01$, $***P < 0.001$ (unpaired *t*-test).

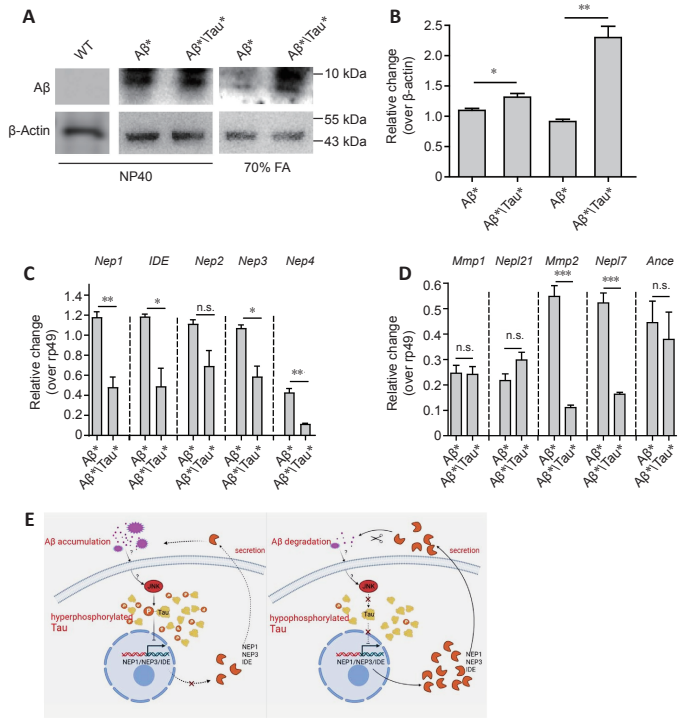

Figure 5 | **Tau reduces amyloid-beta (Aβ) degradation in the *Drosophila* model.**
(A) Soluble and insoluble Aβ levels were analyzed by western blot using an anti-Aβ antibody. Actin was used as the loading control. ELAV-Gal4 was used to drive Tau* and Aβ* expression in the fly central nervous system (CNS). Western blots were repeated three times, and a representative blot is shown. (B) Quantitative results for panel A; the Aβ level was normalized to actin. (C and D) RT-PCR analysis of the mRNA expression levels of genes encoding Aβ-degrading enzymes (Additional Table 1); *dNep1*, *dNep2*, *dNep3*, *dNep4*, *dIDE*, *dMmp1*, *dMmp2*, *dNepl7*, *dNepl21* and *dAnce* mRNA levels were analyzed by RT-PCR, and rp49 was used as the loading control. Statistical differences were determined from the band intensities, which were analyzed by ImageJ software. The intensity of each band was normalized to the intensity of rp49. ELAV-Gal4 was used to drive Tau* and Aβ* expression in the fly CNS. Data are presented as the mean ± SEM. $*P < 0.05$, $**P < 0.01$, $***P < 0.001$ (unpaired *t*-test). n.s.: Not significant. (E) A model depicting the reciprocal interaction between Aβ and Tau toxicity. 1) Toxicity of Aβ is dependent on tau hyperphosphorylation. 2) The hypophosphorylated tau mutant is not affected by Aβ. Aβ accumulation activates JNK and results in the hyperphosphorylation and accumulation of tau. Tau can also block the mRNA expression of the Aβ-degrading enzymes *Nep1*, *Nep3*, *Nep4*, *Mmp2*, and *IDE*, which may block the clearance of Aβ and result in the aggravation of Aβ accumulation and toxicity. This reciprocal interaction loop further accelerates AD progression and pathology.

Yoshida et al., 2004; Lagalwar et al., 2006). In our study, inhibition of JNK activity by SP600125 significantly reduced tau toxicity, which was aggravated by Aβ. Although the Aβ-JNK-Tau cascade can be established, the underlying mechanism of Aβ-induced JNK activation is still unclear. Indeed, JNK can be activated by several stimuli (Mehan et al., 2011). Some of these stimuli are related to AD pathology. For example, oxidative stress can specifically activate JNK and is also prevalent in the AD brain. In our experiments, we used vitamin C to reduce oxidative stress in Aβ co-expressed flies. Vitamin C partially eliminated tau hyperphosphorylation induced by Aβ, which was accompanied by a reduction in JNK activity (**Additional Figure 3A** and **B**). These data suggest that oxidative stress was one of the mediators that contributed to Aβ-induced JNK activation and tau hyperphosphorylation; however, the detailed mechanism still requires further investigation. Aβ can cause oxidative stress in several other models (Shelat et al., 2008; Cheignon et al., 2018). Oxidative stress may induce the oxidation of Trx1 and JNK inhibitory protein, which in turn may lead to the activation of JNK (Han et al., 2009). Aβ can induce ER stress signaling (Fonseca et al., 2013), which can lead to JNK activation (Fonseca et al., 2013) through activation of the transmembrane protein kinase IRE1 (Urano et al., 2000). DNA damage response pathways can also be activated by Aβ (Santiard-Baron et al., 2001), resulting in subsequent JNK activation (Hamdi et al., 2005). Furthermore, alterations in inflammatory cytokines released from microglia in the AD brain have been reported to activate JNK (Wang et al., 2015).

Our results suggest that Aβ and tau toxicities can be reciprocally aggravated. Aβ can aggravate tau hyperphosphorylation and toxicity, and, reciprocally, tau can aggravate Aβ deposition. This Aβ-JNK-Tau-Aβ loop will accelerate the progression of AD. In fact, supporting our findings in the fly model, the formation of Aβ plaques in mice can also be enhanced by tau (Jackson et al., 2016), and Aβ can significantly promote tau aggregation (He et al., 2018).

Aβ(Arc2E) expression in the fly can cause a severe phenotype as previously described (Crowther et al., 2005), including rough eye and degeneration. However, our results showed that Aβ(Arc2E) expression did not induce a rough eye phenotype, and we suspected that the expression level of Aβ in our Aβ(Arc2E) flies was lower than the previously used fly line. To test this possibility, we expressed Aβ(Arc2E) in fly eyes using high-temperature conditions (29°C). Our results indicated that Aβ(Arc2E) caused a rough eye phenotype at 29°C but not at 25°C; moreover, Aβ(Arc2E) also aggravated the rough eye phenotype at 29°C (**Additional Figure 4**).

As described, Aβ and tau can work synergistically (Folwell et al., 2010). Aβ expression can synergistically enhance several phenotypes caused by tau expression, such as disruption of axonal transport and the neuromuscular junction related to synaptic dysfunction (Folwell et al., 2010). Aβ and tau protein can interact synergistically through the direct interaction between the R2 domain of tau and Aβ oligomers, leading to the acceleration of protein aggregation (Miller et al., 2011). The synergistic interaction between Aβ and tau was indeed involved in and contributed to the neuropathology in an AD animal model (Clinton et al., 2010).

How tau aggravates Aβ accumulation is unclear. Our results indicate that tau can reduce the mRNA expression of genes encoding Aβ-degrading enzymes, including *dNep1*, *dNep3*, *dMmp2*, *dNep4*, and *dIDE*. It is likely that tau can interfere with the processing of Aβ. According to our results, the level of *dBace1* mRNA, which encodes an APP cleaving enzyme, was increased, but the mRNA level of the presenilin gene dPsn was reduced when Tau* was co-expressed with Aβ* (**Additional Figure 5**). However, this result needs to be investigated further. As described, tau protein can be found in the nucleus and is related to heterochromatin stability. The level of nuclear hyperphosphorylated tau is associated with stress stimulation. In particular, the ribosomal DNA transcriptional repression-related protein TIP5 is associated with tau protein, and this association may result in the regulation and suppression of gene transcription (Maina et al., 2018). Tau aggregates can also be associated with U2 snRNA, which can regulate gene expression and harbor transcription-related RNAs and proteins (Galganski et al., 2017). Therefore, besides the disruption of neuronal function, such as the interference in axon transport and neurotransmitter release, pathological tau may also decrease the expression of genes related to Aβ clearance. As a consequence, Aβ and tau can reciprocally intensify the protein accumulation of each other in AD. This reciprocal loop between Aβ and tau further accelerates and aggravates AD and may cause the variation in AD pathology. This reciprocal relationship between Aβ and tau should be considered and investigated for development of future AD treatments.

Limitations

Although some of the results were repeated using the HEK293 cells, the majority of results in the current study were generated from the *Drosophila* model. The mammalian system is more complex than *Drosophila*, and our results will require confirmation in higher-order model organisms. We propose that Aβ and tau can be considered as a combined target for drug development. However, the mechanisms by which Aβ induces JNK activation and tau inhibits the expression of genes for Aβ-degrading enzymes will require the use of biochemical and-omics approaches in the future.

Conclusion

By using the *Drosophila* AD model, we found that Aβ and tau can reciprocally aggravate their toxicities and promote disease progression through the respective activation of JNK and inhibition of the expression of Aβ-degrading enzymes.

Acknowledgments: *We are grateful to the Bloomington Drosophila Stock Center for fly stocks, the Biomedical Analysis Center of Tsinghua University and the Biomedical Analysis Center of Hangzhou Institute for Advanced Study for their help and services, Dr. Bing-Wei Lu of Stanford University and Dr. Yi Zhong of Tsinghua University for their kind gifts of the flies and reagents. We also thank Zhi-Qing Wang and Wen-Jia Qiang of Tsinghua University for their technical helps.*

Author contributions: *YPH, BZ, and JRW designed the experiments. YPH, ZDS and JXH performed the experiments. YPH analyzed data and wrote the manuscript. All authors approved the final version of the manuscript.*

Conflicts of interest: *The authors declare that there is no conflict of interest.*

Availability of data and materials: *All data generated or analyzed during this study are included in this published article and its supplementary information files.*

Open access statement: *This is an open access journal, and articles are distributed under the terms of the Creative Commons AttributionNonCommercial-ShareAlike 4.0 License, which allows others to remix, tweak, and build upon the work non-commercially, as long as appropriate credit is given and the new creations are licensed under the identical terms.*

Open peer reviewer: *Mohammad Moshahid Khan, University of Tennessee Health Science Center, USA.*

Additional files:

Additional file 1: *Open peer review report 1.*

Additional Figure 1: *Approach to co-expression Tau* and Aβ* in fly eyes and CNS.*

Additional Figure 2: *Amyloid-beta (Aβ)-induced JNK activation in HEK293 cells.*

Additional Figure 3: *Vitamin C eliminates amyloid-beta (Aβ)-induced tau hyperphosphorylation.*

Additional Figure 4: *Aβ(Arc2E) causes rough eye phenotype and aggravate tau toxicity at 29°C.*

Additional Figure 5: *Tau alerts dPsn and dBace mRNA expression in flies.*

Additional Table 1: *Homologues of amyloid-beta (Aβ)-degrading enzymes on the fly genome.*

References

Ballatore C, Lee VM, Trojanowski JQ (2007) Tau-mediated neurodegeneration in Alzheimer's disease and related disorders. Nat Rev Neurosci 8:663-672.

Bilen J, Bonini NM (2005) Drosophila as a model for human neurodegenerative disease. Annu Rev Genet 39:153-171.

Bloom GS (2014) Amyloid-β and tau: the trigger and bullet in Alzheimer disease pathogenesis. JAMA Neurol 71:505-508.

Cao M, Liu F, Ji F, Liang J, Liu L, Wu Q, Wang T (2013) Effect of c-Jun N-terminal kinase (JNK)/p38 mitogen-activated protein kinase (p38 MAPK) in morphine-induced tau protein hyperphosphorylation. Behav Brain Res 237:249-255.

Carson JA, Turner AJ (2002) Beta-amyloid catabolism: roles for neprilysin (NEP) and other metallopeptidases? J Neurochem 81:1-8.

Cerro-Herreros E, Chakraborty M, Pérez-Alonso M, Artero R, Llamusí B (2017) Expanded CCUG repeat RNA expression in Drosophila heart and muscle trigger Myotonic Dystrophy type 1-like phenotypes and activate autophagocytosis genes. Sci Rep 7:2843.

Chakrabarti S, Khemka VK, Banerjee A, Chatterjee G, Ganguly A, Biswas A (2015) Metabolic risk factors of sporadic Alzheimer's disease: implications in the pathology, pathogenesis and treatment. Aging Dis 6:282-299.

Cheignon C, Tomas M, Bonnefont-Rousselot D, Faller P, Hureau C, Collin F (2018) Oxidative stress and the amyloid beta peptide in Alzheimer's disease. Redox Biol 14:450-464.

Chen GF, Xu TH, Yan Y, Zhou YR, Jiang Y, Melcher K, Xu HE (2017) Amyloid beta: structure, biology and structure-based therapeutic development. Acta Pharmacol Sin 38:1205-1235.

Chen G, Chen KS, Knox J, Inglis J, Bernard A, Martin SJ, Justice A, McConlogue L, Games D, Freedman SB, Morris RG (2000) A learning deficit related to age and beta-amyloid plaques in a mouse model of Alzheimer's disease. Nature 408:975-979.

Clinton LK, Blurton-Jones M, Myczek K, Trojanowski JQ, LaFerla FM (2010) Synergistic Interactions between Abeta, tau, and alpha-synuclein: acceleration of neuropathology and cognitive decline. J Neurosci 30:7281-7289.

Crowther DC, Kinghorn KJ, Miranda E, Page R, Curry JA, Duthie FA, Gubb DC, Lomas DA (2005) Intraneuronal Abeta, non-amyloid aggregates and neurodegeneration in a Drosophila model of Alzheimer's disease. Neuroscience 132:123-135.

Dias-Santagata D, Fulga TA, Duttaroy A, Feany MB (2007) Oxidative stress mediates tau-induced neurodegeneration in Drosophila. J Clin Invest 117:236-245.

Foidl BM, Humpel C (2020) Can mouse models mimic sporadic Alzheimer's disease? Neural Regen Res 15:401-406.

Folwell J, Cowan CM, Ubhi KK, Shiabh H, Newman TA, Shepherd D, Mudher A (2010) Abeta exacerbates the neuronal dysfunction caused by human tau expression in a Drosophila model of Alzheimer's disease. Exp Neurol 223:401-409.

Fonseca AC, Ferreiro E, Oliveira CR, Cardoso SM, Pereira CF (2013) Activation of the endoplasmic reticulum stress response by the amyloid-beta 1-40 peptide in brain endothelial cells. Biochim Biophys Acta 1832:2191-2203.

Fortini ME, Skupski MP, Boguski MS, Hariharan IK (2000) A survey of human disease gene counterparts in the Drosophila genome. J Cell Biol 150:F23-30.

Galganski L, Urbanek MO, Krzyzosiak WJ (2017) Nuclear speckles: molecular organization, biological function and role in disease. Nucleic Acids Res 45:10350-10368.

Gistelinck M, Lambert JC, Callaerts P, Dermaut B, Dourlen P (2012) Drosophila models of tauopathies: what have we learned? Int J Alzheimers Dis 2012:970980.

Goedert M, Hasegawa M, Jakes R, Lawler S, Cuenda A, Cohen P (1997) Phosphorylation of microtubule-associated protein tau by stress-activated protein kinases. FEBS Lett 409:57-62.

Goyal D, Ali SA, Singh RK (2021) Emerging role of gut microbiota in modulation of neuroinflammation and neurodegeneration with emphasis on Alzheimer's disease. Prog Neuropsychopharmacol Biol Psychiatry 106:110112.

Hamdi M, Kool J, Cornelissen-Steijger P, Carlotti F, Popeijus HE, van der Burgt C, Janssen JM, Yasui A, Hoeben RC, Terleth C, Mullenders LH, van Dam H (2005) DNA damage in transcribed genes induces apoptosis via the JNK pathway and the JNK-phosphatase MKP-1. Oncogene 24:7135-7144.

Han D, Ybanez MD, Ahmadi S, Yeh K, Kaplowitz N (2009) Redox regulation of tumor necrosis factor signaling. Antioxid Redox Signal 11:2245-2263.

He Z, Guo JL, McBride JD, Narasimhan S, Kim H, Changolkar L, Zhang B, Gathagan RJ, Yue C, Dengler C, Stieber A, Nitla M, Coulter DA, Abel T, Brunden KR, Trojanowski JQ, Lee VM (2018) Amyloid-β plaques enhance Alzheimer's brain tau-seeded pathologies by facilitating neuritic plaque tau aggregation. Nat Med 24:29-38.

Hensley K, Floyd RA, Zheng NY, Nael R, Robinson KA, Nguyen X, Pye QN, Stewart CA, Geddes J, Markesbery WR, Patel E, Johnson GV, Bing G (1999) p38 kinase is activated in the Alzheimer's disease brain. J Neurochem 72:2053-2058.

Hoover BR, Reed MN, Su J, Penrod RD, Kotilinek LA, Grant MK, Pitstick R, Carlson GA, Lanier LM, Yuan LL, Ashe KH, Liao D (2010) Tau mislocalization to dendritic spines mediates synaptic dysfunction independently of neurodegeneration. Neuron 68:1067-1081.

Hu Y, Sopko R, Foos M, Kelley C, Flockhart I, Ammeux N, Wang X, Perkins L, Perrimon N, Mohr SE (2013) FlyPrimerBank: an online database for Drosophila melanogaster gene expression analysis and knockdown evaluation of RNAi reagents. G3 (Bethesda) 3:1607-1616.

Huang Y, Wu Z, Zhou B (2015) hSOD1 promotes tau phosphorylation and toxicity in the Drosophila model. J Alzheimers Dis 45:235-244.

Huang Y, Wu Z, Cao Y, Lang M, Lu B, Zhou B (2014) Zinc binding directly regulates tau toxicity independent of tau hyperphosphorylation. Cell Rep 8:831-842.

Ittner LM, Ke YD, Delerue F, Bi M, Gladbach A, van Eersel J, Wölfing H, Chieng BC, Christie MJ, Napier IA, Eckert A, Staufenbiel M, Hardeman E, Götz J (2010) Dendritic function of tau mediates amyloid-beta toxicity in Alzheimer's disease mouse models. Cell 142:387-397.

Jackson RJ, Rudinskiy N, Herrmann AG, Croft S, Kim JM, Petrova V, Ramos-Rodriguez JJ, Pitstick R, Wegmann S, Garcia-Alloza M, Carlson GA, Hyman BT, Spires-Jones TL (2016) Human tau increases amyloid β plaque size but not amyloid β-mediated synapse loss in a novel mouse model of Alzheimer's disease. Eur J Neurosci 44:3056-3066.

Jeon Y, Lee JH, Choi B, Won SY, Cho KS (2020) Genetic dissection of Alzheimer's disease using Drosophila models. Int J Mol Sci 21:884.

Lagalwar S, Guillozet-Bongaarts AL, Berry RW, Binder LI (2006) Formation of phospho-SAPK/JNK granules in the hippocampus is an early event in Alzheimer disease. J Neuropathol Exp Neurol 65:455-464.

Lang M, Fan Q, Wang L, Zheng Y, Xiao G, Wang X, Wang W, Zhong Y, Zhou B (2013) Inhibition of human high-affinity copper importer Ctr1 orthologous in the nervous system of Drosophila ameliorates Aβ42-induced Alzheimer's disease-like symptoms. Neurobiol Aging 34:2604-2612.

Lei P, Ayton S, Bush AI (2021) The essential elements of Alzheimer's disease. J Biol Chem 296:100105.

Link CD (2005) Invertebrate models of Alzheimer's disease. Genes Brain Behav 4:147-156.

Ma QL, Yang F, Rosario ER, Ubeda OJ, Beech W, Gant DJ, Chen PP, Hudspeth B, Chen C, Zhao Y, Vinters HV, Frautschy SA, Cole GM (2009) Beta-amyloid oligomers induce phosphorylation of tau and inactivation of insulin receptor substrate via c-Jun N-terminal kinase signaling: suppression by omega-3 fatty acids and curcumin. J Neurosci 29:9078-9089.

Madabattula ST, Strautman JC, Bysice AM, O'Sullivan JA, Androschuk A, Rosenfelt C, Doucet K, Rouleau G, Bolduc F (2015) Quantitative analysis of climbing defects in a Drosophila model of neurodegenerative disorders. J Vis Exp:e52741.

Maina MB, Bailey LJ, Wagih S, Biasetti L, Pollack SJ, Quinn JP, Thorpe JR, Doherty AJ, Serpell LC (2018) The involvement of tau in nucleolar transcription and the stress response. Acta Neuropathol Commun 6:70.

Mamun AA, Uddin MS, Mathew B, Ashraf GM (2020) Toxic tau: structural origins of tau aggregation in Alzheimer's disease. Neural Regen Res 15:1417-1420.

Mehan S, Meena H, Sharma D, Sankhla R (2011) JNK: a stress-activated protein kinase therapeutic strategies and involvement in Alzheimer's and various neurodegenerative abnormalities. J Mol Neurosci 43:376-390.

Miller Y, Ma B, Nussinov R (2011) Synergistic interactions between repeats in tau protein and Aβ amyloids may be responsible for accelerated aggregation via polymorphic states. Biochemistry 50:5172-5181.

Miners JS, Baig S, Palmer J, Palmer LE, Kehoe PG, Love S (2008) Abeta-degrading enzymes in Alzheimer's disease. Brain Pathol 18:240-252.

Mitchell K, Iadarola MJ (2010) RT-PCR analysis of pain genes: use of gel-based RT-PCR for studying induced and tissue-enriched gene expression. Methods Mol Biol 617:279-295.

Newman M, Wilson L, Camp E, Verdile G, Martins R, Lardelli M (2010) A zebrafish melanophore model of amyloid beta toxicity. Zebrafish 7:155-159.

Nishimura I, Yang Y, Lu B (2004) PAR-1 kinase plays an initiator role in a temporally ordered phosphorylation process that confers tau toxicity in Drosophila. Cell 116:671-682.

Oh SY, He F, Krans A, Frazer M, Taylor JP, Paulson HL, Todd PK (2015) RAN translation at CGG repeats induces ubiquitin proteasome system impairment in models of fragile X-associated tremor ataxia syndrome. Hum Mol Genet 24:4317-4326.

Ossenkoppele R, Schonhaut DR, Schöll M, Lockhart SN, Ayakta N, Baker SL, O'Neil JP, Janabi M, Lazaris A, Cantwell A, Vogel J, Santos M, Miller ZA, Bettcher BM, Vossel KA, Kramer JH, Gorno-Tempini ML, Miller BL, Jagust WJ, Rabinovici GD (2016) Tau PET patterns mirror clinical and neuroanatomical variability in Alzheimer's disease. Brain 139(Pt 5):1551-1567.

Ploia C, Antoniou X, Sclip A, Grande V, Cardinetti D, Colombo A, Canu N, Benussi L, Ghidoni R, Forloni G, Borsello T (2011) JNK plays a key role in tau hyperphosphorylation in Alzheimer's disease models. J Alzheimers Dis 26:315-329.

Prüßing K, Voigt A, Schulz JB (2013) Drosophila melanogaster as a model organism for Alzheimer's disease. Mol Neurodegener 8:35.

Qiu WQ, Walsh DM, Ye Z, Vekrellis K, Zhang J, Podlisny MB, Rosner MR, Safavi A, Hersh LB, Selkoe DJ (1998) Insulin-degrading enzyme regulates extracellular levels of amyloid beta-protein by degradation. J Biol Chem 273:32730-32738.

Rissman RA, Poon WW, Blurton-Jones M, Oddo S, Torp R, Vitek MP, LaFerla FM, Rohn TT, Cotman CW (2004) Caspase-cleavage of tau is an early event in Alzheimer disease tangle pathology. J Clin Invest 114:121-130.

Santiard-Baron D, Lacoste A, Ellouk-Achard S, Soulié C, Nicole A, Sarasin A, Ceballos-Picot I (2001) The amyloid peptide induces early genotoxic damage in human preneuron NT2. Mutat Res 479(1-2):113-120.

Schneider CA, Rasband WS, Eliceiri KW (2012) NIH Image to ImageJ: 25 years of image analysis. Nat Methods 9:671-675.

Schwabe T, Srinivasan K, Rhinn H (2020) Shifting paradigms: The central role of microglia in Alzheimer's disease. Neurobiol Dis 143:104962.

Shelat PB, Chalimoniuk M, Wang JH, Strosznajder JB, Lee JC, Sun AY, Simonyi A, Sun GY (2008) Amyloid beta peptide and NMDA induce ROS from NADPH oxidase and AA release from cytosolic phospholipase A2 in cortical neurons. J Neurochem 106:45-55.

Shulman JM, Feany MB (2003) Genetic modifiers of tauopathy in Drosophila. Genetics 165(3):1233-42.

Sowade RF, Jahn TR (2017) Seed-induced acceleration of amyloid-β mediated neurotoxicity in vivo. Nat Commun 8:512.

Srivastava S, Ahmad R, Khare SK (2021) Alzheimer's disease and its treatment by different approaches: A review. Eur J Med Chem 216:113320.

Tatebayashi Y, Planel E, Chui DH, Sato S, Miyasaka T, Sahara N, Murayama M, Kikuchi N, Yoshioka K, Rivka R, Takashima A (2006) c-jun N-terminal kinase hyperphosphorylates R406W tau at the PHF-1 site during mitosis. FASEB J 20:762-764.

Tyagi E, Fiorelli T, Norden M, Padmanabhan J (2013) Alpha 1-antichymotrypsin, an inflammatory protein overexpressed in the brains of patients with Alzheimer's disease, induces Tau hyperphosphorylation through c-Jun N-terminal kinase activation. Int J Alzheimers Dis 2013:606083.

Urano F, Wang X, Bertolotti A, Zhang Y, Chung P, Harding HP, Ron D (2000) Coupling of stress in the ER to activation of JNK protein kinases by transmembrane protein kinase IRE1. Science 287:664-666.

van der Kant R, Goldstein LSB, Ossenkoppele R (2020) Amyloid-β-independent regulators of tau pathology in Alzheimer disease. Nat Rev Neurosci 21:21-35.

Wang WY, Tan MS, Yu JT, Tan L (2015) Role of pro-inflammatory cytokines released from microglia in Alzheimer's disease. Ann Transl Med 3:136.

Wei W, Norton DD, Wang X, Kusiak JW (2002) Abeta 17-42 in Alzheimer's disease activates JNK and caspase-8 leading to neuronal apoptosis. Brain 125(Pt 9):2036-2043.

Wittmann CW, Wszolek MF, Shulman JM, Salvaterra PM, Lewis J, Hutton M, Feany MB (2001) Tauopathy in Drosophila: neurodegeneration without neurofibrillary tangles. Science 293:711-714.

Yamazaki Y, Zhao N, Caulfield TR, Liu CC, Bu G (2019) Apolipoprotein E and Alzheimer disease: pathobiology and targeting strategies. Nat Rev Neurol 15:501-518.

Yao M, Nguyen TV, Pike CJ (2005) Beta-amyloid-induced neuronal apoptosis involves c-Jun N-terminal kinase-dependent downregulation of Bcl-w. J Neurosci 25:1149-1158.

Yoshida H, Hastie CJ, McLauchlan H, Cohen P, Goedert M (2004) Phosphorylation of microtubule-associated protein tau by isoforms of c-Jun N-terminal kinase (JNK). J Neurochem 90:352-358.

Zempel H, Thies E, Mandelkow E, Mandelkow EM (2010) Abeta oligomers cause localized Ca(2+) elevation, missorting of endogenous Tau into dendrites, Tau phosphorylation, and destruction of microtubules and spines. J Neurosci 30:11938-11950.

Zhang T, Ma S, Lv J, Wang X, Afewerky HK, Li H, Lu Y (2021) The emerging role of exosomes in Alzheimer's disease. Ageing Res Rev 68:101321.

Zeng L, Jiang HL, Ashraf GM, Li ZR, Liu R (2021) MicroRNA and mRNA profiling of cerebral cortex in a transgenic mouse model of Alzheimer's disease by RNA sequencing. Neural Regen Res 16:2099-2108.

Zhu X, Raina AK, Rottkamp CA, Aliev G, Perry G, Boux H, Smith MA (2001) Activation and redistribution of c-jun N-terminal kinase/stress activated protein kinase in degenerating neurons in Alzheimer's disease. J Neurochem 76:435-441.

C-Editor: Zhao M; S-Editor: Li CH; L-Editors: Li CH, Song LP; T-Editor: Jia Y

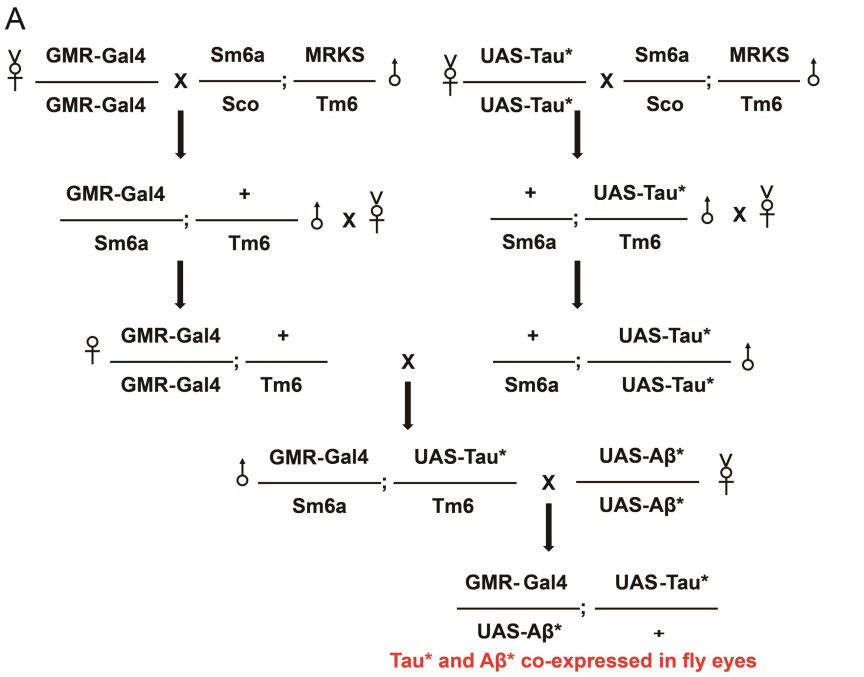

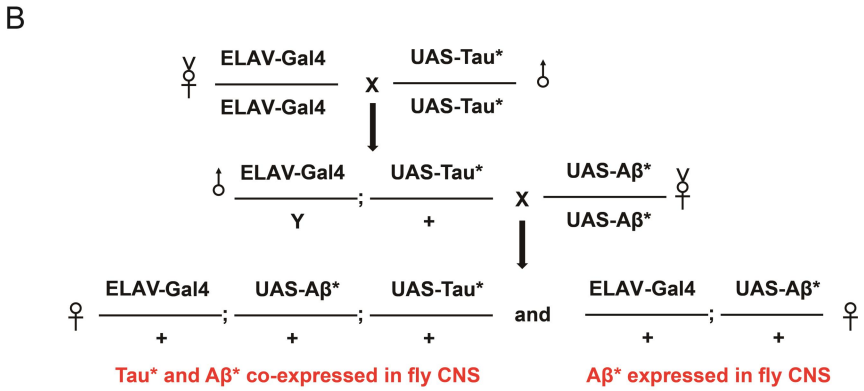

Additional Figure 1 Approach to co-expression Tau* and Aβ* in fly eyes and the central nervous system.

(A) The approach to generate flies with Tau(R406W) (indicated as Tau*) and Aβ(Arc2E) (indicated as Aβ*) co-expression in compound eyes. The final genotype is Gmr-Gal4\UAS-Aβ*; UAS-Tau*\+. (B) The approach to generate flies with Tau* and Aβ* co-expression in fly central nervous system (CNS). The final genotype is Elav-Gal4\+; UAS-Aβ*\+; UAS-Tau*\+. Aβ: Amyloid-beta.

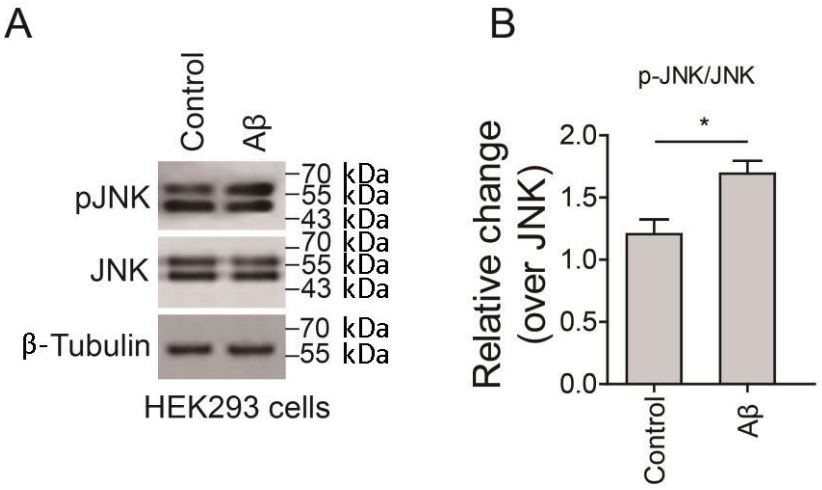

Additional Figure 2 Amyloid-beta (Aβ)-induced JNK activation in HEK293 cells.

(A) Western blot analysis of the level of p-JNK in HEK293 cells with Tau(R406W)-RFP (indicated as Tau*-RFP) expression. Tau*-RFP cells were treated with 10 μM $A\beta_{40}$ peptide for 24 hours and further treated with 1 μM SP600125 for 6 hours. WB results were repeated three times and the representative results were shown here. (B) The quantitative result of A. Western blot results were calculated using ImageJ software. The level of p-JNK was normalized to JNK. Data are presented as the mean ± SEM. *$P < 0.05$ (unpaired *t*-test).

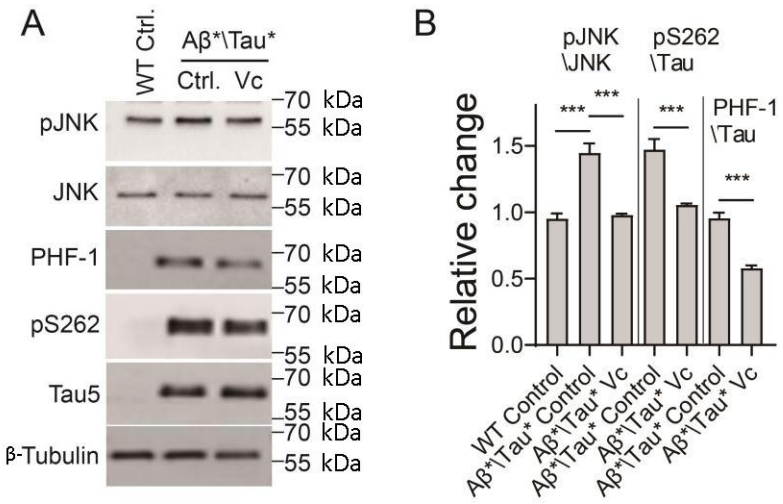

Additional Figure 3 Vitamin C eliminates amyloid-beta (Aβ)-induced tau hyperphosphorylation.

(A) Western blot analysis of the levels of p-JNK and hyperphosphorylated tau in flies. GMR-Gal4 was used to drive Tau(R406W) (indicated as Tau*) and Aβ(Arc2E) (indicated as Aβ*) co-expression in fly eyes, flies were treated with Vitamin C (Vc). WB results were repeated three times, and only one of the results was shown here. (B) The quantitative result of A. The level of p-JNK was normalized to JNK. One-way analysis of variance was used for comparison of three groups (in comparison with the means of pre-selected pairs of columns). Levels of pS262 and PHF-1 were normalized to Tau5 signal. Data are presented as the mean ± SEM. ***$P < 0.001$ (unpaired *t*-test). WT Ctrl.: Wild-type control.

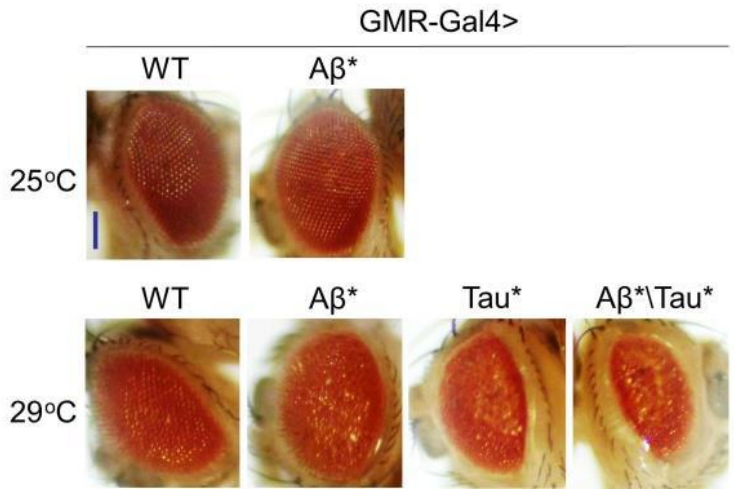

Additional Figure 4 Aβ(Arc2E) causes rough eye phenotype and aggravate tau toxicity at 29°C.
Images of the compound eyes from Aβ(Arc2E) and Aβ(Arc2E)\Tau(R406W) flies at 29°C. GMR-Gal4 was used to drive Aβ(Arc2E) and Tau(R406W) expression in the compound eyes. Scale bar: 100μm. Aβ: Amyloid-beta.

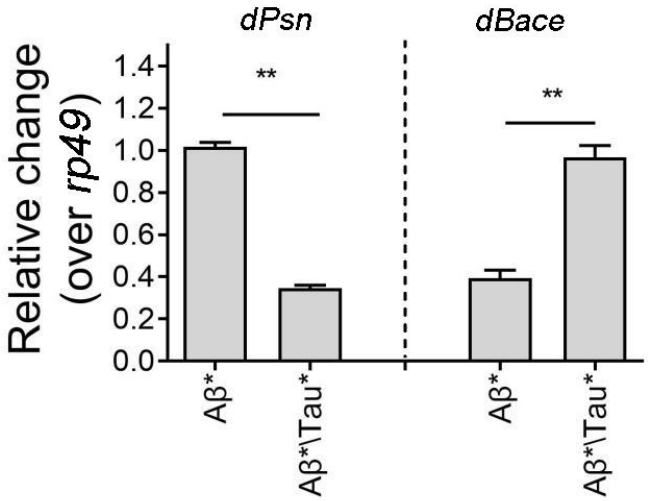

Additional Figure 5 Tau alerts *dPsn* and *dBace* mRNA expression in flies.

The mRNA expression levels of *dPsn* and *dBace* in Aβ*\Tau* co-expression flies were analyzed by the gel-based reverse transcription PCR, rp49 was used as the loading control. The intensities of bands were quantitated using ImageJ software and normalized to the signal of *rp49*. ELAV-Gal4 was used to drive Tau* and Aβ* expression in fly central nervous system. Data are presented as the mean ± SEM. $^{**}P < 0.01$ (unpaired *t*-test). Aβ: Amyloid-beta.